Human Fall Detection Using mmWave Radars: A Cluster-Assisted Experimental Approach

Charalampos K. Armeniakos[1*], Viktor Nikolaidis[1†], Vasileios Tsekenis[1†], Konstantinos Maliatsos[1†], Petros S. Bithas[2†] and Athanasios G. Kanatas[1†]

[1*]Department of Digital Systems, School of ICT, University of Piraeus, Piraeus, 18534, Greece.

[2]General Department, National and Kapodistrian University of Athens, Athens, 15772, Greece.

*Corresponding author(s). E-mail(s): harmen@unipi.gr;
Contributing authors: vnikola@unipi.gr; vtsekenis@gmail.com; kmaliat@unipi.gr; pbithas@uoa.gr; kanatas@unipi.gr;
[†]These authors contributed equally to this work.

Abstract

Accurate and timely human fall detection is a strong requirement either for the surveillance of critical infrastructures or for ships. Indeed, sea-faring vessels are one of the most important means for maintaining the marine economy in many countries by transporting goods or people. However, unfortunate tragic accidents on-board ships involving people, either a member of the ship's crew or a passenger who has fallen off the ship may take place, which is known by the term "man overboard" (MOB). Accordingly, the use of radar sensors for human safety monitoring applications is vital and is of special interest since it is proven that radar sensors are less influenced by environmental conditions (e.g. fog, rain, temperature) compared to other systems like video cameras. Consequently, human fall detection from either sea or ground infrastructures is easier to be identified using radars compared to the conventional methods. This paper focuses in the description of a real experimental approach based on multiple long-range millimeter-wave band radar sensors for human fall detection. The stream(s) of information collected by the system, are processed using clustering techniques. The clustering results are evaluated in terms of the ability to detect and track real human fall scenarios. The results reveal that the measure of velocity plays a key role in the detection procedure.

Keywords: Man Overboard, Automotive radar, mmWave radar, human fall detection, measurements, IoT, clustering techniques, k-means, Gaussian mixture model

1 Introduction

In the past few years, the detection of human fall as a result of accidental or deliberate activity has been identified of major importance for surveillance systems. In this context, a very important aim of the International Maritime Organizations (IMO) is saving the life of passengers and crew on board ship in an emergency situation, as a consequence of either a more general shipping accident or a more specific MOB case according to the recommendation of ITU-R M.2285-0 (2013). Specifically, in cruise ships, approximately 22 people fall off the ship each year while 79% of them do not survive or are considered missing (Örtlund and Larsson, 2018). Trying to portray the broader view, an estimate of more than 1000 people are involved in MOB incidents yearly (Feraru et al, 2020) while the survival rate of such incidents being extremely low. Thus, MOB is clearly a critical event that demands immediate handling with fast detection being the most crucial factor, for the quickest and most efficient recovery of the victim.

The use of radar sensors for human safety monitoring and detection applications is a widely researched topic in recent years. This is even more vital and of special interest for sea-faring vessels and MOB cases, since it is proven that radars are less influenced by environmental conditions, e.g. fog, rain or similar adverse weather conditions, in contrast with other systems such as video or thermal cameras. Nonetheless, detecting humans using any kind of sensor system is a challenging task due to the wide variety of positions and appearances which humans can assume. It is even more challenging considering the case of a ship in motion, along with its' sensors, having on-board stationary or moving people with completely unpredictable behavior very often, whom in case of an MOB incident they will be found in sea level in the matter of seconds. Other common human detection applications include the recognition of human fall from ground infrastructures and detection of fence intrusion (Yousefi et al, 2008). Towards this direction, in Bhadwal et al (2019), the authors propose a surveillance system utilizing a Wireless Sensor Network (WSN) and computer vision technology. Similarly, the authors in Berrahal et al (2016), propose a cooperative border surveillance solution composed of WSNs and unmanned aircraft vehicles (UAVs). All the above summarize why most of the studies have been based on other sensors, e.g. video, thermal, infrared cameras & laser scanners.

1.1 Related Work

In the bibliography we encounter similar approaches that have been employed and proposed in this context. In Sevin et al (2016), the authors use a WSN to detect a MOB incident while the developed system in Örtlund and Larsson (2018) is comprised of transceivers using Long Range (LoRa) techniques and the aid of an artificial intelligence (AI) system with deep learning capabilities. Similarly, in Sheu et al (2020), LoRa Access Points (APs) were used where the authors proposed a complementary dynamic GPS tracking and monitoring system, consisting of wearable sensing aids and physical electric fences, all under a centralized control system. RGB[1] and thermal sensors can be found in Katsamenis et al (2020), where the possibilities and limitations of vision-based systems are discussed. In Zhang et al (2020), the authors propose a novel object detection and tracking method of moving objects with unmanned surface vehicles. Subsequently, the proposed model is evaluated with data obtained by the camera and the laser radar and verified through real experimentation in a river. In Jeong et al (2018), the authors propose a new deep belief network model for radar signal classification of real marine radar signals. The authors showed that the proposed model performs efficiently in noisy environment and thus enhancing the detection and identification of the targets.

On another front, clustering of measurement data is important, especially in the case of radar signal processing, where the need of detection points clustering becomes obvious while using high-resolution radar sensor systems. In most cases, clustering is often used as a preprocessing step for classification of the measured data. Currently, there is a plethora of work that focuses on clustering techniques of radar data, mainly for automotive radar sensors (Stolz et al, 2018; Li et al, 2018; Scheiner et al, 2019). In Stolz et al (2018), a novel approach for automotive radar data clustering is presented, while an adaptive clustering approach based on a range/angle/velocity-grid generated originally from the radar signal processing and angle estimation stage for automotive high resolution radar sensors is presented in Li et al (2018). In contrast to Stolz et al (2018); Li et al (2018), the authors in Scheiner et al (2019), present a novel approach by first and foremost filtering out static

[1] RGB sensors capture visible light and recognise/detect the colour of a material in RGB (red, green, blue) scale, while rejecting the unwanted infrared or ultraviolet light

background data before applying a two-stage clustering approach on data collected by automotive radar sensors. In (Zhao and Su, 2017), a novel vehicle detection method is proposed by utilizing the Gaussian mixture model (GMM) in order to cluster the radar data to segment foreground targets from the clutter background. In Scheel and Dietmayer (2019), a variational radar model for vehicles is presented. The measurement model is learned from actual data using variational Gaussian mixtures and avoids excessive manual engineering. The authors demonstrate the approach on experimental data, and it is shown that the data-driven measurement model outperforms a manually designed model.

However, all these works focus on the detection of moving targets in traffic scenes. To date and to the best of the authors' knowledge, this is the first time that clustering of experimental radar data such as coordinates & velocity are utilized for the detection & tracking of an MOB scenario.

1.2 Contributions

In this work, clustering techniques are utilized for the first time on an extended set of experimental radar data for the detection & tracking of MOB scenarios. To this end, the k-means and GMM algorithm are exploited for clustering of the collected radar data, related to distance & velocity. Different clustering options of the data are compared to gain semantic insight and the role of velocity in the detection procedure is highlighted. Also, the data retrieval procedure is presented.

The paper is organized as follows. Section 2 describes the system architecture, the topology of the sensors, along with the measurement equipment. In Section 3 the structure of the retrieved radar data is described. Section 4 provides the clustering analysis applied on the dataset. Section 5 provides the clustering results and the comparison of the algorithms in terms of the ability to detect a human fall. In Section 6 the concluding remarks can be found.

2 System Architecture & Measurement Setup

A Radar (radio detection and ranging) is a detection system for objects, enclosing additional information such as range, velocity and angle, based on electromagnetic waves in the radiofrequency spectrum extending from around 3MHz to 110GHz (3mm to 100m). Waves in this frequency range are characterized by only weak interactions with dust, fog, rain and falling snow. Thus, radars become ideal for detecting objects in the field, even under extreme weather conditions. Common applications are in air, marine and terrestrial traffic control (speed controls), in meteorology (weather radars), in earth science (Ground Penetrating Radar or GPR), in astronomy (radio telescopes) as well as in the automobile industry (Adaptive Cruise Control or ACC).

The measurement scenarios were all conducted in the Nikaia Olympic Weightlifting Hall which is part of the University campus. This building was reserved for the needs of the measurement campaign and provided an ideal setup for the MOB simulations. It is noted that the balcony was constructed in such a way, with metal grid mesh floor and metal railings, that provided a realistic representation of a ship's floor and gunwale. The measurement scenarios that were planned to be executed involved throwing a human-shaped doll from the balcony of the second floor of the building, as it appears in Figure 1.

Fig. 1: Radar configuration measurement setup

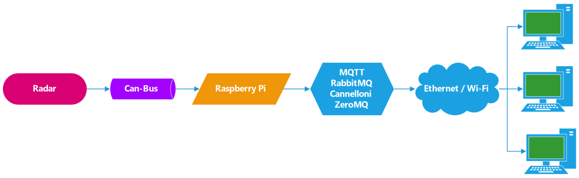

Fig. 2: System Topology

The system comprises of multiple Continental's ARS 408-21 (Continental Engineering Services, 2018) long range radar sensors that operate in the frequency spectrum of 76-77GHz. In our experiments, the first radar (R1) is placed 14m above the ground facing downwards whereas the second (R2) is facing sideways and is placed in a position where its projection on the vertical and horizontal axis, regarding R1, is 4 and 6 meters away respectively. This can be seen in Figure 1 where the topology of the two sensors is depicted. During the experiments, a human-shaped doll, 1,60m tall and weighing 40 Kgs, was guided to perform free fall from a position 3-6 meters below R1 and 2 meters adjacent to R2, as seen in Figure 1.

This type of radar has two scanning modes, while in operation surveying the area under consideration, performing a scan in the short (SR) and far range (FR) at each measurement cycle. In the short range, the sensor covers a distance ranging from 0.20m to 70m/100m with azimuth & elevation angle Field of View (FoV) of $\pm 60°$& 20°respectively and 0.20m to 250m with a FoV of $\pm 9°/14°$in the far range accordingly. In both modes, the distance measuring accuracy is high, ± 0.10m and ± 0.40m, in the short and far range respectively, while the velocity range is -400km/h to 200km/h, for leaving and approaching objects with a measuring accuracy of 0.1km/h.

These sensors are connected in the system via a serial connection interface using the Controller Area Network (CAN) bus standard specification. Each sensor is connected to a Raspberry Pi 3+ microcontroller with an add-on extension board (PiCAN2) that provides CAN bus interface capability. The microcontroller is responsible for the bus initialization and the overall operation of the sensor via special commands in hexadecimal values of the form "CAN_ID #CAN_MSG". The CAN_ID specifies the type of configuration setup while the CAN_MSG denotes the specific parameter(s) that will be configured via this message eventually. Each radar is connected via this high speed (500 kbit/s) CAN bus interface with the host microcontroller (Raspberry Pi) and is capable of transmitting a full set of measurements, in both short and far range, every 70-80ms approximately. The data, can then be forwarded to a single or multiple computer (or computing infrastructures), more powerful than the microcontroller, that will carry on the additional post processing. This can be implemented in various ways either using a publisher/subscriber model such as MQTT, RabbitMQ and ZeroMQ, or by using a more custom approach with CANnelloni (Reinhardt et al, 2015). CANnelloni[2] implements a Socket-based CAN over Ethernet tunnel, in Linux operating systems (OS), in order to transfer CAN frames between two machines using UDP[3] packets. Figure 2, presents the configuration setup described above and summarizes the system architecture used throughout the measurements.

Table 1: List of CAN ID messages

CAN ID	**Content**
0x200	Radar sensor configuration
0x201	Radar status
0x600	Cluster status (list header)
0x700	Software Version Identification
0x701	Cluster general information
0x702	Cluster quality information

3 Data Retrieval

The radars are configured to operate in "Cluster mode", providing information data such as position, velocity and radar cross section (RCS) for each cluster found. Each such cluster is synonymous to a single point or entity discovered in the surrounding area. The position of each cluster is given in a Cartesian coordinate system relative to the position of the sensor, as shown in Figure 3, while the velocity is calculated relatively to the sensor's speed (if it is mounted in a moving platform, either a vehicle or a ship). A full measurements scan is comprised of various CAN messages, as they appear in Table 1, each holding a specific piece of information. The measurement cycle starts with a hexadecimal CAN_ID message [0x600] (or "Cluster status") which denotes the beginning of the frame, along with the number of clusters identified during the full scan in both modes, short and far range. Immediately afterwards follows the messages that carry the cluster general and quality information with CAN_ID

[2]The source code repository at GitHub is available at https://github.com/mguentner/cannelloni

[3] User Datagram Protocol (UDP), is part of the Internet protocol (IP) for low-latency communication and loss-tolerating connections over the Internet

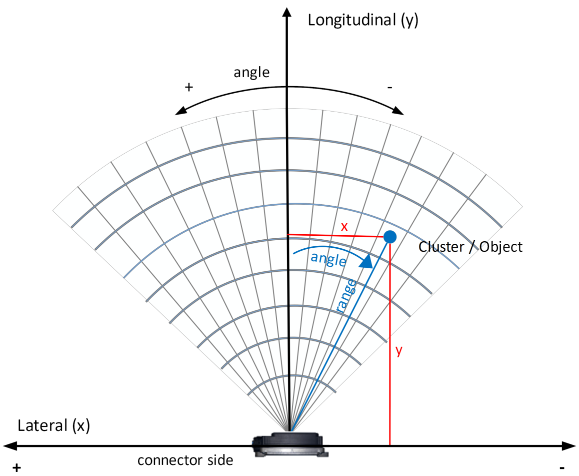

Fig. 3: Radar coordinate system

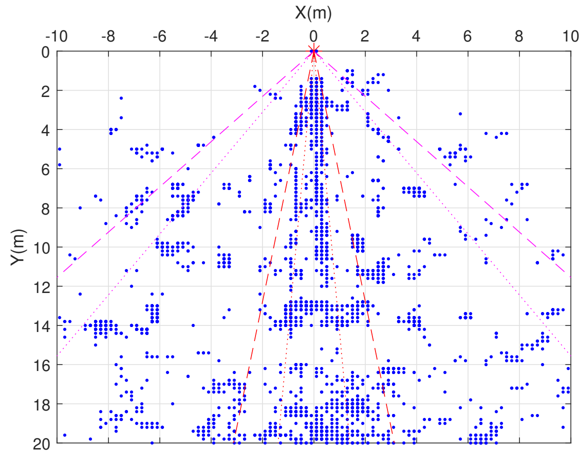

Fig. 4: Indicative measurement of an area of interest (AoI). The red asterisk reveals the location of the sensor

[0x701] and [0x702][4] respectively. Each [0x701] message contains the position, velocity and the RCS of a cluster and is sent repeatedly for all the detected clusters (first SR scan, then FR scan) in that cycle. Figure 4 depicts all the clusters found after a measurement scan in an area of 20x20m, which forms the Area of Interest (AoI), with the clusters' coordinates being relative to the sensor's location (0,0). The AoI, which can differ in shape and size, forms an indicative area that is monitored more closely and constantly given the overall area that is covered by the sensors.

In addition to the clusters' location, the sensor quality information is forwarded also for all identified clusters. The information that can be extracted, help someone to identify and discard clusters that are not valid, ambiguous, stationary or artefacts. This elimination process of the unwanted clusters discovered per measurement cycle, reduces the load of post-processing by the machine learning, or any other algorithms applied, and increases the chance of identifying a target with higher accuracy. Indicatively, the clusters that are mainly taken in consideration during the post processing belong to one of the following categories i) Valid, ii) Valid Low RCS, iii) Valid Azimuth Correction, iv) Valid No Local Maximum, v) Valid Suspicious Angle, and vi) Valid High Child Probability. With this in mind, in Figure 5 we can distinguish valid and invalid clusters after a measurement scan. The blue and red dots denote the valid and invalid clusters respectively, while the green dot at (0,0) specifies the location of the sensor.

[4]The CAN_ID messages [0x702] carrying clusters' quality information are not sent by default, and this option must be activated manually.

4 Clustering Analysis

In this section, the utilization of k-means and GMM algorithm on real extracted radar measurement data, is presented. In particular, the clustering concept of the obtained radar data is analytically described. Subsequently, three clustering scenarios based on different measures, are analyzed.

4.1 k-means Analysis and Setup

In this subsection, the clustering procedure of data with the k-means algorithm, is described. The extracted radar data from each measurement scenario are separated into a total number of N time snapshots they feed as input to k-means algorithm. In this analysis, the k-means algorithm is fed with the measures of coordinates (position) and velocity of the preprocessed captured data. It is noted that the snapshot analysis of the captured radar data and all the preprocessing steps are beyond the scope of this paper.

The k-means algorithm performs clustering of the input data in order to separate the samples of the data (observations) into k groups (clusters).

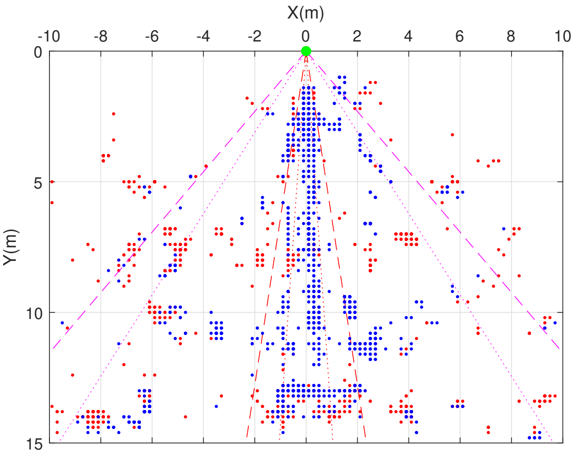

Fig. 5: Indicative measurement scan of an AoI with the blue & red dots representing valid & invalid clusters respectively, and the green dot the location of the sensor

Note that the clusters formed by k-means algorithm are not to be confused with the clusters (points) extracted by the radar. For the rest of the analysis, the clusters formed by the k-means algorithm will be referred to as groups. The output of the algorithm provides the samples of the measures as well as the centroids of each group formed. In short, the steps of k-means algorithm which applied to the retrieved radar data are described as follows:

Step 1. Choose initial k for the center (centroids) of the groups. Generally, the initialization is arbitrary. Alternatively, the k-means++ algorithm (Chapelle et al, 2006) can be utilized for cluster center initialization.

Step 2. Compute the distances between the centers of the groups and the samples of each observation. Let $\mathbf{x}$ be a set of observations and $\mathbf{S} = \{S_1, S_2, \ldots, S_k\}$ a set of k groups with $\boldsymbol{\mu}_k$ denoting the centers of the samples at S_k. Then, the goal is to minimize the metric $\sum\limits_{\mathbf{x}\in\mathbf{S}_i} \|\mathbf{x}-\boldsymbol{\mu}_i\|^2$. The minimization of this metric can be performed in terms of the Hamming distance, correlation distance, Euclidean distance etc. In this work, the square of the Euclidean distance was utilized for the execution of k-means algorithm.

Step 3. There are two ways to proceed:
- Batch update - Assign each observation to the group with the closest centroid.
- Online update - Individually assign observations to a different centroid if the reassignment decreases the sum of the within-group sum-of-squares (WCSS) point-to-group-centroid distances $\underset{\mathbf{S}}{argmin} \sum\limits_{i=1}^{k} \sum\limits_{\mathbf{x}\in\mathbf{S}_i} \|\mathbf{x}-\boldsymbol{\mu}\|^2$.

In this work, the batch update method is considered.

Step 4. Compute the average of the observations in each group to obtain k new centroid locations.

Step 5. Repeat steps 2 through 4 until group assignments do not change, or the maximum number of iterations is reached. In this k-means algorithm, a maximum number of 100 iterations is considered.

The assignment for the appropriate value of k is dynamic and it is not performed manually. In particular, for a given range of the values of k, the algorithm considers every single value among a maximum number of K groups. Each value is separately evaluated in order for the optimal k to be selected. In this analysis, the optimal value of k is selected through the silhouette criterion (Kaufman and Rousseeuw, 1990), which is a simple and effective method for finding the optimal k. A high silhouette value indicates that an observation is well matched to its own group, and poorly matched to other group. The value of k that is found to contain the highest average silhouette value, is chosen to be fed as input to the k-means algorithm.

Once the appropriate k has been selected, the observations from the measures of distance and velocity are fed into the k-means algorithm individually or as a combination. The goal is to evaluate the k-means algorithm upon the extracted preprocessed radar data and obtain insight and semantic information for MOB-related scenarios.

4.2 Feeding the k-means Algorithm

In this subsection, the feeding procedure of the preprocessed radar data on k-means algorithm, is described. In particular, the effect of the distance and velocity measure on the clustering procedure is captured separately and jointly. To the

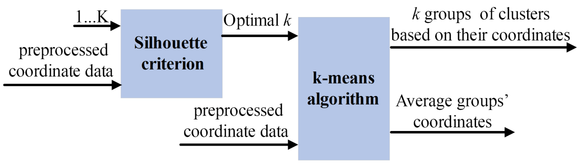

Fig. 6: Flow diagram of the distance-based k-means clustering

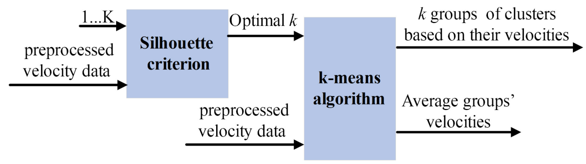

Fig. 7: Flow diagram of the velocity-based k-means clustering

best of the authors' knowledge, this is the first time that the effect of different measures such as the distance and velocity on the extraction of semantic information for human fall detection from sea and ground infrastructures, is captured for experimental radar data. Accordingly, the k-means algorithm is described for the three cases of the feeding procedure that have been identified.

4.2.1 Distance-based k-means Clustering

In this case, the k-means algorithm accepts as input the coordinates of the preprocessed data of an AoI. In particular, the feeding procedure can be performed for only one measurement snapshot or for a given set of snapshots. A predefined range of consecutive snapshots defines a window of length L snapshots in time. For a desired given window, the AoI is defined and the preprocessing of the coordinates of the clusters is performed. In this way, it is possible to extract and analyze the obtained radar data for different snapshots over a whole measurement scenario.

Next, the coordinates of all clusters which are contained in a given window are evaluated based on the silhouette criterion. In particular, for a given range of the values of k, exhaustive search is executed and the optimal value for k is selected. Subsequently, the k-means algorithm is executed upon the coordinates data for the optimal value of k, according to the procedure described in the subsection 4.1. The overall procedure is depicted in Figure 6.

4.2.2 Velocity-based k-means Clustering

In this case, the k-means algorithm accepts as input the velocities of the preprocessed clusters of an AoI. In particular, during the feeding procedure of the k-means algorithm, the velocities of the preprocessed clusters obtained by the radar, are

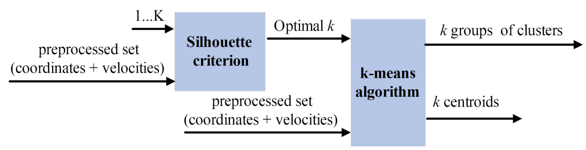

Fig. 8: Flow diagram of the distance- and velocity-based k-means clustering

extracted for a given set of snapshots. Following the same procedure as previously, the silhouette criterion is applied on the preprocessed velocity data and the optimal value of k is found. The k-means algorithm is now executed for the optimal value of k. As an output of the algorithm, K groups of clusters are formed based on the velocity of the clusters. The average group velocity is also obtained. The overall procedure that was described is depicted in Figure 7.

4.2.3 Distance- & Velocity-based k-means Clustering

In this case, the k-means algorithm accepts as input both the coordinates and the velocities of the preprocessed clusters of an AoI. The overall set which is fed to the k-means algorithm now consists of the preprocessed clusters' coordinates and velocities for a given AoI. The set which is formed, is evaluated through the silhouette criterion in order for the optimal k to be obtained. Next, the k-means algorithm is executed for the optimal value of k. As an output of the algorithm, k groups of clusters are formed by considering both the coordinates and the velocities of the input set. The centroids of the k groups are also obtained. The overall procedure that was described is depicted in Figure 8.

4.3 Gaussian mixture model

In this subsection, the basic principles of the Gaussian mixture model (GMM) clustering, are

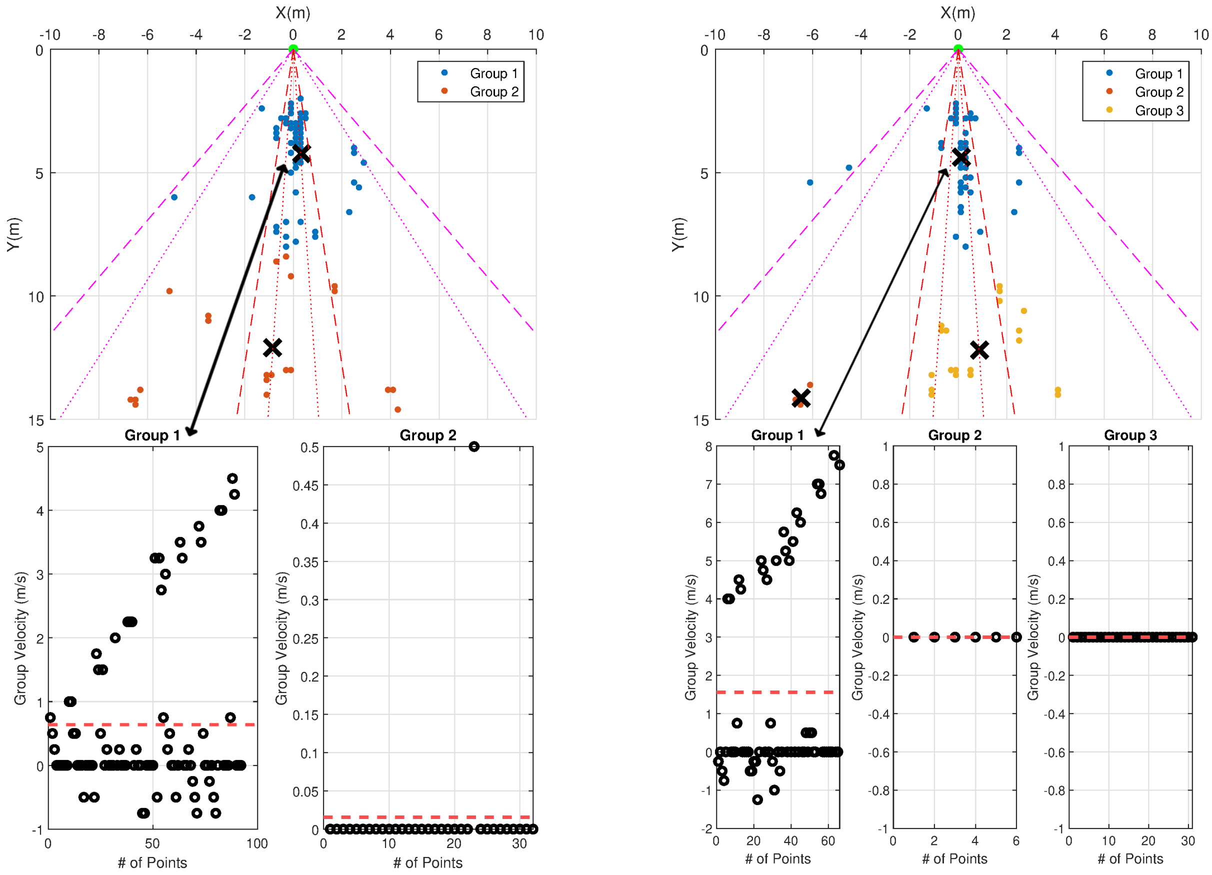

(a) (b)

Fig. 9: Illustration of the groups that formed after applying k-means clustering upon the clusters' coordinates of a window, for (a) the 1st window and (b) the 2nd window

presented. GMM can be used to group the data in much the same way as k-means by assuming that the data follow Gaussian distribution. However, since GMM is a distribution-based clustering method, the model output is not a hard assignment of points to specific groups. Instead, the algorithm is based on the probability that a point belongs to a Gaussian distribution (group). Subsequently, the parameters of each Gaussian $\boldsymbol{\theta}$ (i.e. variance/covariance, mean and weight) need to be addressed in order to cluster the measurement data, but first the knowledge of which sample belongs to what Gaussian, is necessary.

This is achieved through the expectation maximization (EM) algorithm. At a high level, the EM algorithm can be described as follows:

Step 1. Initialize random Gaussian parameter $\boldsymbol{\theta}$.

Step 2. Proceed to the following:

a) Expectation Step: Compute $\mathbb{P}[x_i = g \mid \boldsymbol{\theta}]$, that is the probability that the sample i came from the group g given the Gaussian parameter vector $\boldsymbol{\theta}$.

b) Maximization Step: Update the Gaussian parameter $\boldsymbol{\theta}$, i.e., recalculate $\boldsymbol{\theta}$ of each group (distribution).

Step 3. Repeat Step 2, until convergence has been achieved.

Similar to the k-means algorithm, the GMM is fed with the measures of coordinates (position) and velocity of the preprocessed captured data and the assignment for the appropriate value of k is achieved through the silhouette criterion. Similar to k-means analysis, the observations from the measures of distance and velocity are fed into the GMM algorithm individually or as a combination in order to obtain semantic information for MOB

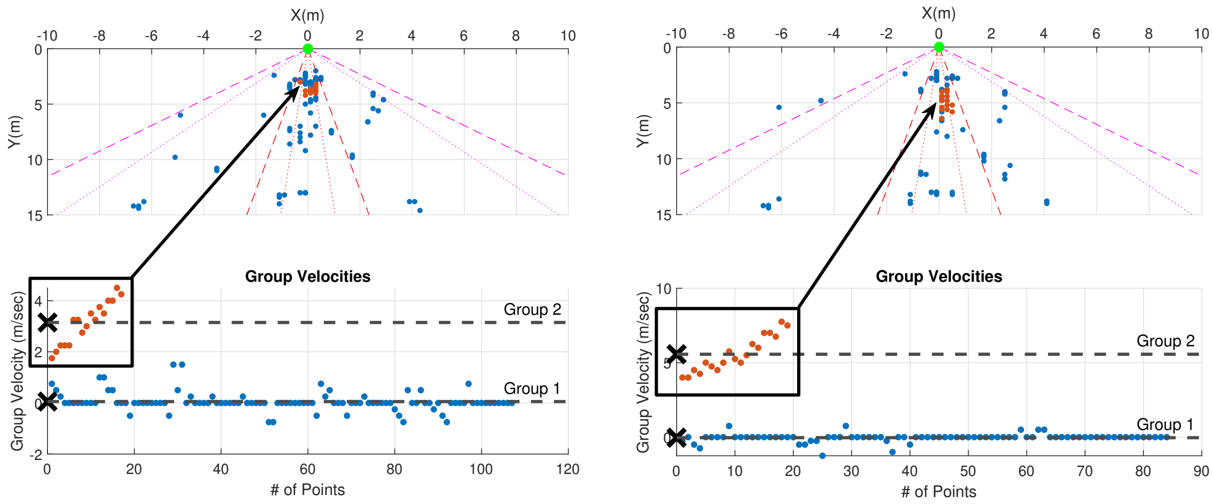

(a) (b)

Fig. 10: Illustration of the groups formed after applying k-means clustering upon the clusters' velocities of a window, for (a) the 1$^{\text{st}}$ window and (b) the 2$^{\text{nd}}$ window

scenarios. The feeding procedure follows the same lines as the one presented in Figs. 6–8, and thus it is omitted here for brevity.

5 Results & Discussion

In this section, the clustering analysis is applied on the experimental preprocessed radar data and it is evaluated in terms of the ability to extract semantic information for a MOB scenarios. The representative measurement scenario that has been chosen to be evaluated through the k-means and GMM clustering involve the throwing of a human-shaped doll from the balcony of the second floor of a building. It is worth mentioning that the measurement campaign fully complies with the ISO/PAS 21195:2018(E) (2018) standard, i.e., the guidelines and regulations in order to emulate realistically a MOB scenario. The radar from which the measurement data have been obtained is R1, as shown in Figure 1. This scenario under evaluation consists of N=290 snapshots. The maximum number of groups that can be formed is set to K=4 and the window for which the clusters have been obtained is L=6. The data of two representative and consecutive windows have been selected to be preprocessed and subsequently to be fed into the clustering algorithms. In the next subsections, the clustering algorithms are evaluated and compared in terms of the ability to detect and track a MOB scenario.

5.1 Impact of Coordinates

In Figure 9, the groups which formed after applying the k-means algorithm upon the coordinates of the clusters, are shown.

The AoI that has been defined is also depicted in Figure 9 and the radar R1 is depicted with green dot. In Figure 9a, two clusters have been formed and consequently k=2. This value was obtained after applying the silhouette criterion on the input data. The centroids of the two groups are also depicted. In Figure 9b, the k-means algorithm is applied on the coordinates of the clusters obtained from the 2$^{\text{nd}}$ window. As shown in Figure 9b, the radar detects new clusters during this range of snapshots. Three groups have now been formed and consequently k=3. It is also observed that 3 new centroids have now been identified.

Notice that in both Figures 9a and 9b, it is possible that a group contains clusters that correspond to the human-shaped doll which is falling. Indeed, after obtaining the corresponding velocities of the clusters from each group, it is observed that in both Figures 9a and 9b, Group 1 consists of some clusters with velocity. The velocities of the groups are shown as a function of the number of clusters. Consequently, it can be concluded

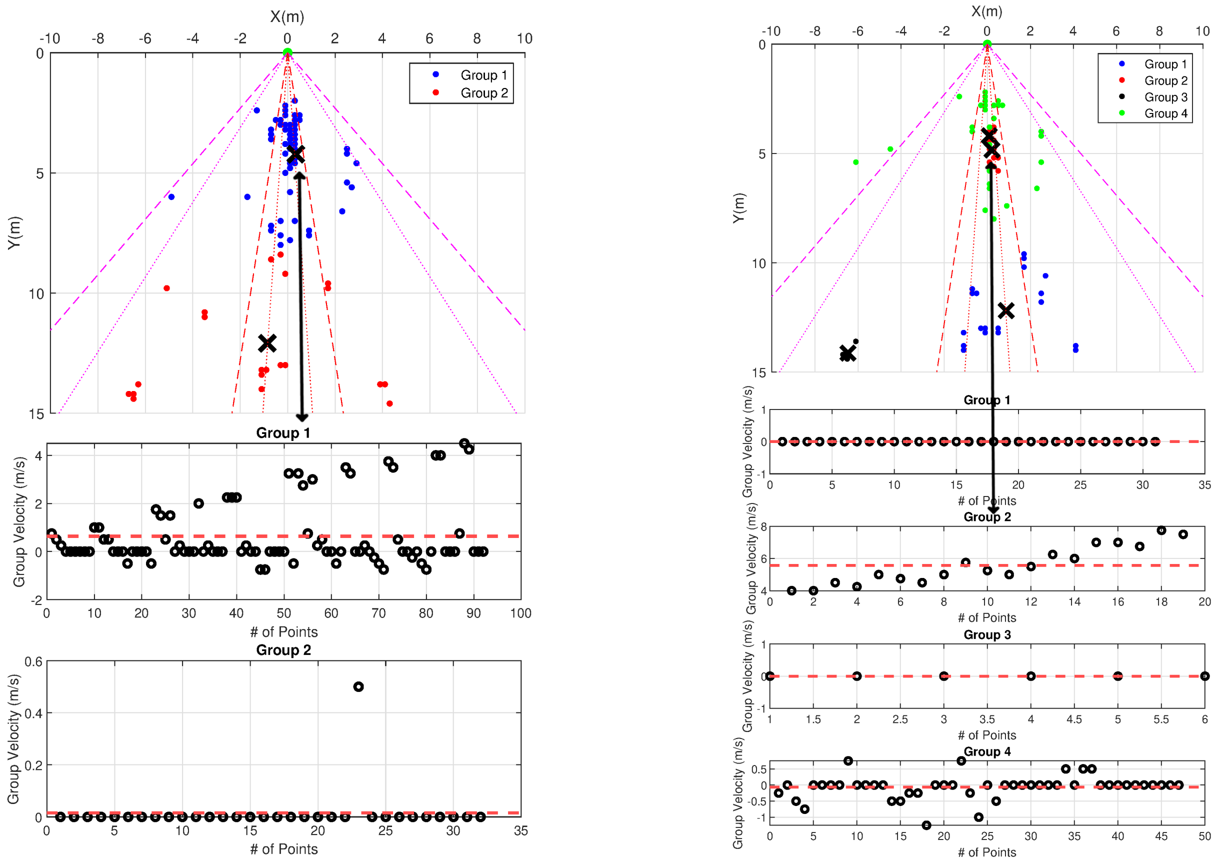

(a) (b)

Fig. 11: Illustration of the groups formed after applying k-means clustering upon the clusters' coordinates and velocities of a window, for (a) the 1st window and (b) the 2nd window

that there is a target within Group 1 for both figures which is most probably falling. Unfortunately, although the average location of Group 1 is known, it is not easy to observe the accurate spot at which the doll is identified upon the coordinate map. The GMM coordinate-based clustering provided almost identical clustering results with the one conducted by k-means and no superiority of GMM over k-means is witnessed. Thus, the GMM coordinate-based clustering results are omitted here for brevity.

5.2 Impact of Velocities

In Figure 10, the groups that have been formed after applying the k-means algorithm on the velocities of the clusters, are illustrated. The average velocity of each group is also shown. The corresponding coordinates of the clusters from each group are identified and depicted upon the coordinate map. Interestingly, notice that in both Figures 10a and 10b, the velocities of the Group 2, correspond to some clusters of the identified falling target, i.e., of the doll. In particular, Figure 10a illustrates the groups' velocities as a function of the number of clusters. The velocities of Group 2 increase linearly and the average velocity is 3 m/sec. The corresponding coordinates of the clusters of the Group 2 for the 1st window are located upon the coordinate map at approximately Y=4m. Consequently, it is observed that some clusters which appear at Y=4m have an increasing speed, as indicated by the velocities of Group 2. In Figure 10b, similar results are observed for the 2nd window. However,

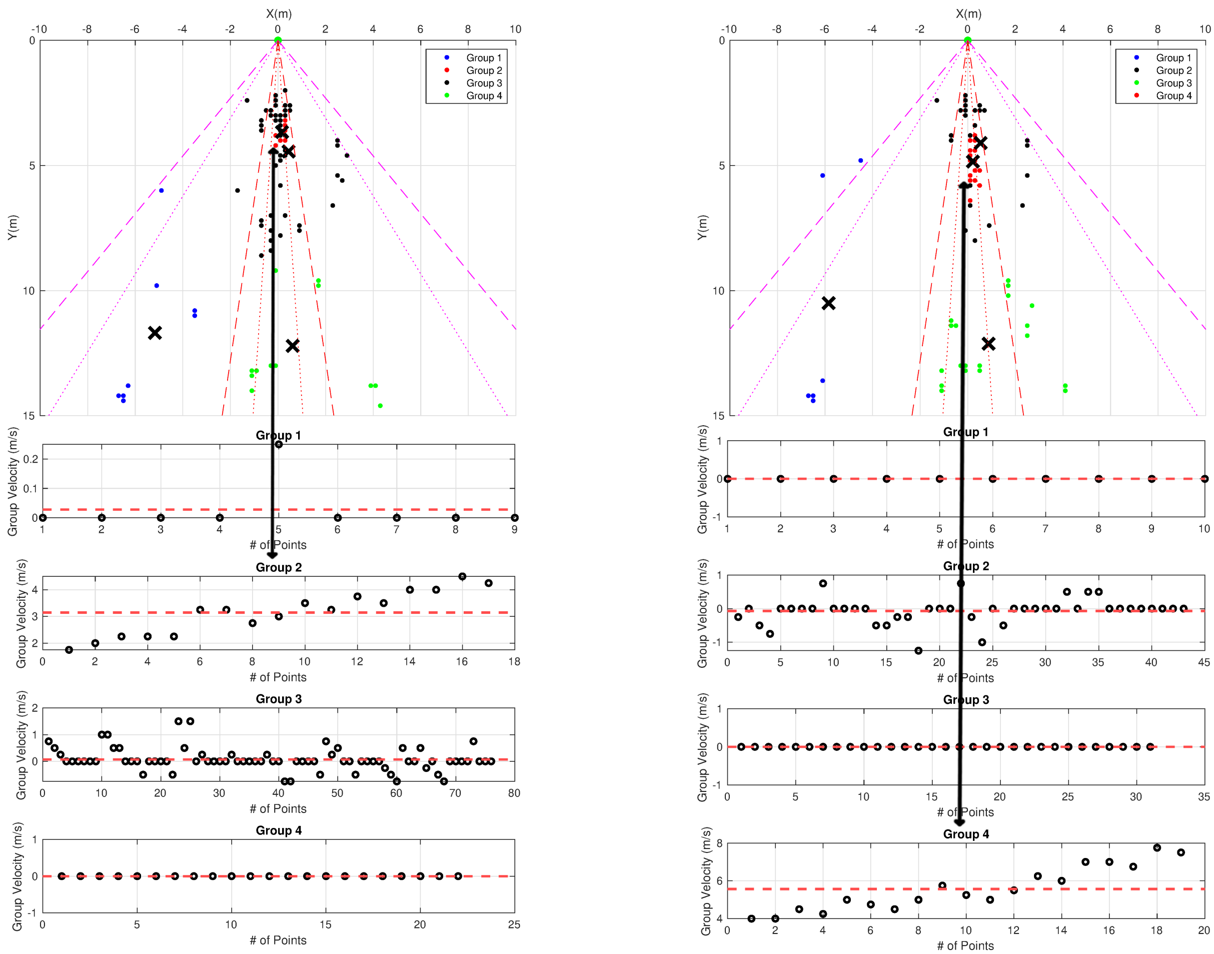

(a) (b)

Fig. 12: Illustration of the groups formed after applying GMM clustering upon the clusters' coordinates and velocities of a window, for (a) the 1$^{\text{st}}$ window and (b) the 2$^{\text{nd}}$ window

in this case, the average velocity of Group 2 is 6 m/sec and the corresponding clusters have now been identified beyond Y=5m upon the coordinate map. In other words, a target which consists of some clusters with increased speed, has been observed. In addition, the average velocity of Group 1 tends to zero for both Figures 10a and 10b, which makes the detection and the tracking of the falling target easily detectable. To conclude, it seems that velocity plays a key role in the detection of a fall although the accurate average position of each group cannot be clearly located. When the clusters' velocities increase, the human fall is clearly tracked in two consecutive windows. The GMM velocity-based clustering, provided almost identical results with the one conducted by k-means and no superiority of GMM over k-means is witnessed. Thus, GMM velocity-based clustering results are omitted here for brevity.

5.3 Impact of both Coordinates and Velocity

In Figure 11, the groups that have been formed after applying the k-means algorithm on both the coordinates and the velocities of the clusters, are illustrated on the coordinate maps. The respective groups of velocities are also depicted.

As one may notice, the clustering that was performed in Figure 11a, is similar to the one performed in Figure 9a. This is because the coordinates of the clusters with velocity, are very close to the centroid of Group 1. In this case, the coordinates of Group 1 seem to affect the clustering more. In other words, Group 1 velocities are not that high in order for the algorithm to form a separate group consisted only of high velocity clusters. However, one can conclude that there is a falling target within Group 1, but it cannot be clearly identified and tracked upon the coordinate map.

In Figure 11b, 4 groups have been formed. Interestingly, although most of the clusters' coordinates of Group 2 and Group 3 are very close, two different groups have been formed. This is because the respective velocities of Group 2 and 3 have very different velocities and k-means is affected more by the measure of velocity. In this case, the high velocity clusters form Group 2, which is located on the coordinate map. Now, the detection and the tracking of the falling target is much easier to be detected, i.e., in Group 2 with centroid at approximately Y=5m it is observed there is a target falling with approximate average velocity of 6 m/sec. The rest of the groups have zero average velocity and thus it can be concluded that no other fall upon the AoI exists.

In Figure 12, the results of GMM clustering using both the clusters' coordinates and velocities of the two consecutive windows are depicted. In both windows, the silhouette criterion implies k=4 groups. The average locations and velocities of the groups are also presented. Surprisingly, in contrast to Figure 11a, the GMM clustering is superior to the one provided by k-means. Indeed, as shown in Figure 12a, the GMM algorithm isolates the clusters with an increasing velocity into Group 2. For the rest of the clusters, the classification seems to be based on their coordinates. In this case, the clusters' coordinates of the group with the highest average velocity, i.e., Group 2, have been located upon the coordinate map and the average location has been accurately identified. In other words, both the average location and the average velocity of the falling human-shaped doll can be observed. Similar to Figure 12a, in Figure 12b, the GMM algorithm isolates the clusters with the highest velocity into Group 4. The corresponding average location of Group 4, is now identified at approximately Y=5m and the tracking of the falling doll between Figure 12a and Figure 12b, is now possible. By comparing Figs. 12a and 12b, it is easy

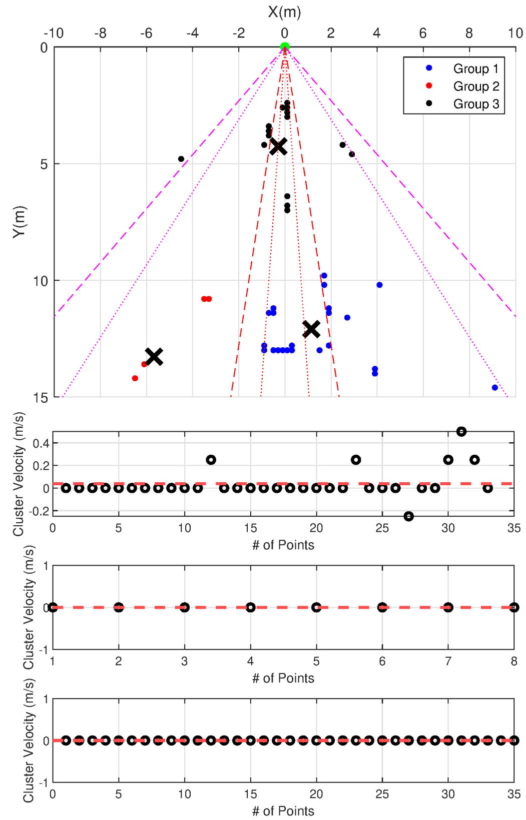

Fig. 13: Illustration of the groups formed after applying k-means clustering upon the clusters' coordinates and velocities of a window, captured after the fall

to observe that the doll is falling and it is now located at approximately Y=5m with an average velocity at approximately 6 m/sec.

For completeness and in order to illustrate the importance of both clustering techniques in the extraction of semantic information about the detection of fall, Figure 13 is presented. In Figure 13, the illustrated 4 groups have been formed after applying the k-means clustering upon the clusters' coordinates and velocities of a window, intentionally taken after the end of the fall. The results derived through GMM are identical to the ones presented with k-means and thus they are omitted. As one can easily observe, all the groups that have been formed have approximately zero average velocity. As the average velocity of all clusters is approximately equal, both k-means and GMM are affected more by the coordinates of the clusters. Notice that most of the groups' clusters are scattered upon the coordinate map and no object can be clearly distinguished. This is in contrast to both Figs. 11a and 11b, where most clusters of the Group 1 and 2, respectively, are gathered around the centroid of each group and consequently, the target is easier to be detected.

6 Conclusions & Future Work

In this paper, the study of a system based on long-range millimeter-wave band radar sensors for human fall detection and tracking based on a real experimental approach, was performed. Subsequently, the k-means and GMM clustering was analyzed and utilized for the extraction of semantic information. To this end, a real measurement scenario was studied, and both k-means and GMM algorithm were applied upon the real measurement radar data and compared to gain insight. It was shown that although the clustering is affected both by the coordinates and the velocities of the clusters, the measure of velocity seems to provide more optimistic results in terms of the detection of human fall. It was shown that, if the clusters are closely related in terms of coordinates, the algorithms are strongly affected by the clusters' velocities. Vice versa, if the clusters are closely related in terms of their velocities, the algorithms are strongly affected by the clusters' coordinates. When both coordinates and velocities were utilized for clustering, the GMM algorithm was superior to k-means algorithm in detecting and tracking the human fall. The results also revealed that the proposed approach contributes to the extraction of semantic information about the detection and tracking of a human fall and the combination of both coordinates and velocities of the clusters seems to be the most insightful.

As a future work, the clustering results of the presented work can be fed into various machine learning algorithms and neural networks as an extra feature of the training data sets, in order to be utilized and tested in a real MOB scenario. A further extension is to configure the proposed clustering algorithms so that they can enable real-time tracking of a human fall scenario.

Acknowledgments. This research has been co-financed by the European Regional Development Fund of the European Union and Greek national funds through the Operational Program Competitiveness, Entrepreneurship and Innovation, under the call "RESEARCH-CREATE-INNOVATE" (Project Code: T1EDK-01169, Project Name: MHTIS).

Declarations

Data Availability Statements

The datasets generated during and/or analysed during the current study are not publicly available due to Non Disclosure Agreement signed by the authors with the partners of the research project but are available from the corresponding author on reasonable request.

Conflict of interest

The authors declare that they have no conflict of interest.

References

Berrahal S, Kim JH, Rekhis S, et al (2016) Border surveillance monitoring using quadcopter UAV-aided wireless sensor networks. Journal of Communications Software and Systems 12(1):67. https://doi.org/10.24138/jcomss.v12i1.92

Bhadwal N, Madaan V, Agrawal P, et al (2019) Smart border surveillance system using wireless sensor network and computer vision. In: 2019 International Conference on Automation, Computational and Technology Management (ICACTM). IEEE, pp 183–190, https://doi.org/10.1109/icactm.2019.8776749

Chapelle O, Scholkopf B, Zien A (2006) Semi-Supervised Learning. The MIT Press

Continental Engineering Services (2018) Continental ARS 408-21 Long Range Radar Sensor 77 GHz. URL https://hexagondownloads.blob.core.windows.net/public/AutonomouStuff/wp-content/uploads/2020/08/ARS-408-21-whitelabel.pdf

Feraru VA, Andersen RE, Boukas E (2020) Towards an autonomous UAV-based system to assist search and rescue operations in man overboard incidents. In: 2020 IEEE International Symposium on Safety, Security, and Rescue Robotics (SSRR), pp 57–64, https://doi.org/10.1109/SSRR50563.2020.9292632

ISO/PAS 21195:2018(E) (2018) Plastics - Ships and marine technology - Systems for the detection of persons while going overboard from ships (Man overboard detection). Standard International Organization for Standardization, Geneva, CH

ITU-R M.2285-0 (2013) Maritime survivor locating systems and devices (man overboard systems), An overview of systems and their mode of operation. Approved in 12-2013, Status : In force (Main)

Jeong CM, Jung YG, Lee SJ (2018) Deep belief networks based radar signal classification system. Journal of Ambient Intelligence and Humanized Computing https://doi.org/10.1007/s12652-018-0774-7

Katsamenis I, Protopapadakis E, Voulodimos A, et al (2020) Man overboard event detection from RGB and thermal imagery. In: Proceedings of the 13th ACM International Conference on PErvasive Technologies Related to Assistive Environments. ACM, pp 1–6, https://doi.org/10.1145/3389189.3397998

Kaufman L, Rousseeuw PJ (eds) (1990) Finding Groups in Data: An Introduction to Cluster Analysis. John Wiley & Sons, Inc., https://doi.org/10.1002/9780470316801

Li M, Stolz M, Feng Z, et al (2018) An adaptive 3D grid-based clustering algorithm for automotive high resolution radar sensor. In: 2018 IEEE International Conference on Vehicular Electronics and Safety (ICVES). IEEE, pp 1–7, https://doi.org/10.1109/icves.2018.8519483

Reinhardt D, Guntner M, Kucera M, et al (2015) Mapping CAN-to-ethernet communication channels within virtualized embedded environments. In: 10th IEEE International Symposium on Industrial Embedded Systems (SIES). IEEE, pp 1–10, https://doi.org/10.1109/sies.2015.7185064

Scheel A, Dietmayer K (2019) Tracking multiple vehicles using a variational radar model. IEEE Transactions on Intelligent Transportation Systems 20(10):3721–3736. https://doi.org/10.1109/tits.2018.2879041

Scheiner N, Appenrodt N, Dickmann J, et al (2019) A multi-stage clustering framework for automotive radar data. In: 2019 IEEE Intelligent Transportation Systems Conference (ITSC). IEEE, pp 2060–2067, https://doi.org/10.1109/itsc.2019.8916873

Sevin A, Bayilmis C, Erturk I, et al (2016) Design and implementation of a man-overboard emergency discovery system based on wireless sensor networks. Turkish Journal of Electrical Engineering and Computer Sciences 24:762–773. https://doi.org/10.3906/elk-1308-154

Sheu BH, Yang TC, Yang TM, et al (2020) Real-time alarm, dynamic GPS tracking, and monitoring system for man overboard. Sensors and Materials 32(1):197. https://doi.org/10.18494/sam.2020.2582

Stolz M, Li M, Feng Z, et al (2018) High resolution automotive radar data clustering with novel cluster method. In: 2018 IEEE Radar Conference (RadarConf18). IEEE, pp 0164–0168, https://doi.org/10.1109/radar.2018.8378550

Yousefi A, Dibazar AA, Berger TW (2008) Intelligent fence intrusion detection system: detection of intentional fence breaching and recognition of fence climbing. In: 2008 IEEE Conference on Technologies for Homeland Security. IEEE, pp 620–625, https://doi.org/10.1109/ths.2008.4635057

Zhang W, Gao XZ, Yang CF, et al (2020) A object detection and tracking method for security in intelligence of unmanned surface vehicles. Journal of Ambient Intelligence and Humanized Computing https://doi.org/10.1007/s12652-020-02573-z

Zhao Y, Su Y (2017) Vehicles detection in complex urban scenes using gaussian mixture model with FMCW radar. IEEE Sensors Journal 17(18):5948–5953. https://doi.org/10.1109/jsen.2017.2733223

Örtlund E, Larsson M (2018) Man Overboard detecting systems based on wireless technology. Chalmers University of Technology, URL https://hdl.handle.net/20.500.12380/256283